Rev. Adv. Mater. Sci. 27 (2011) 165-172

MICROSTRUCTURE OF NANOCRYSTALLINE WC POWDERS AND WC-Co HARD ALLOYS

A.S. Kurlov[1], A. Leenaers[2], S. van den Berghe[2], M. Scibetta[2], H. Schröttner[3] and A.A. Rempel[1]

[1]Institute of Solid State Chemistry, Ural Division of the RAS, 620990 Ekaterinburg, Russia
[2]SCK-CEN, NMS Institute, 2400 Mol, Belgium
[3]Institute for Electron Microscopy and Fine Structure Research, Graz University of Technology, 8010 Graz, Austria

Received: August 06, 2010

Abstract. A set of WC-Co hard alloys was sintered from WC powders with different mean particle sizes. WC powders with particles having different mean size were prepared by high-energy ball milling and by plasma-chemical synthesis. The microstructure and mean grain size of sintered WC-Co hard alloy specimens were studied by means of SEM and XRD. Vickers hardness and microhardness of sintered WC-Co hard alloys were measured. The mechanical strength of rods prepared from different WC-Co hard alloys was examined by bending tests. After the bending tests, the fracture surfaces of all specimens were studied by SEM.

1. INTRODUCTION

The melting point of hexagonal tungsten carbide WC is equal to ~2790 °C which is less than melting point of nonstoichiometric TiC, ZrC, HfC, NbC, and TaC carbides [1,2]. Hardness of tungsten carbide WC is equal to 18-22 GPa at room temperature which is less than that of nonstoichiometric TiC_y, ZrC_y, HfC_y, VC_y, NbC_y, and TaC_y carbides [1,2]. However, the hardness of WC is sufficiently stable in a wide temperature interval. For example, the microhardness H_V of hexagonal WC carbide decreased from ~18 to ~12 GPa at heating from room temperature to 1000 °C [3] whereas H_V of nonstoichiometric transition metal carbides decreased under the same conditions from their maximum values to 3-8 GPa. Tungsten carbide WC has Young's modulus $E \approx 700$ GPa [2,4,5] which is twice as large as Young's modulus of other carbides. A thermal expansion coefficient of WC is equal to ~$5.5 \cdot 10^{-6}$ K^{-1} [4,5] and is half as much as that of other transition metal carbides.

The mentioned properties of WC and especially their thermal stability during the heating up to 700-900 °C determine an application of WC carbide as the basis for producing of wear-resistant hard alloys. The direct use of WC carbide as cutting tool material is impossible because of its brittleness and sintering at very high temperatures. For this reason, a metallic binder is usually added to tungsten carbide, which insures the required strength of the material without significant reducing its hardness. A binding metal is required to prevent formation of carbides. Melted binder is required to wet WC grains well. Partial solubility of WC in binding metal is necessary too because it provides their strong adhesion. In the case of tungsten carbide WC, best of all these requirements are met by cobalt Co.

The ternary system W–Co-C and especially its pseudobinary section "tungsten carbide - cobalt" are

Corresponding author: A.S. Kurlov, e-mail: kurlov@ihim.uran.ru

the basic for the industrial production of hard alloys with superior mechanical properties and cutting performance [6,7]. For last 20 years, the production of different substances and materials in nanocrystalline state with grain (particle) size from 20 to 100 nm develops intensively [8,9].

The use of nanocrystalline WC powder as a component of hard alloys is the most perspective way for the production of nanostructured hard alloys having fine-grained microstructure, reduced sintering temperature, high hardness, strength and fracture toughness. Therefore a lot of investigations are devoted to the comparison of the mechanical properties of nanostructured WC based hard alloys with respect to properties of standard hard alloys with micron or submicron grain sizes. Nevertheless, up to now it is not clear whether nanostructured tungsten carbide based hard alloys can replace the standard material in a wide application field. There is no literature data on interrelation of the particle size of WC powder used for sintering of alloy with the grain size and mechanical properties of the hard alloy produced.

In the literature there is large number of papers which are devoted to the nanostructured WC-Co hard alloys. However the results of these works cannot be compared because the hard alloys were prepared from different precursors and more over by different technologies. Thus it is not clear whether the positive or negative effects on the alloy properties achieved in these works are results of fine microstructure or the result of technological parameters used in these works. That is why in present paper the attempt to get comparable results on nanostructured WC-Co hard alloys is undertaken. For this reason the identical regime of sintering is applied for the preparation of WC-8 wt.% Co hard alloys starting from powder precursors with different size of particles.

Thus, the objective of the present paper is to study the influence of particle size of WC powder in micro- and nanoscale on the microstructure, hardness and bending strength of sintered TC8 hard alloys identical in composition to widespread WC-8wt.%Co hard alloys (here and henceforth the designation TC8 means powder mixture or hard alloy with composition WC-8wt.% Co).

2. EXPERIMENTAL

WC-8wt.% Co hard alloys are prepared using four tungsten carbide powders differing in particle size: (1) coarse-grained commercial tungsten carbide WC with mean particle size of 6 μm; (2) submicrocrystalline commercial tungsten carbide WC with mean particle size of about 150 nm; (3) nanocrystalline carbide WC with mean particle size of 60 nm, produced by plasma-chemical synthesis; and (4) nanocrystalline carbide WC with mean particle size of 20 nm, produced by high-energy ball milling of coarse-grained commercial tungsten carbide. A mean particle size of used Co powder is equal to 2 μm.

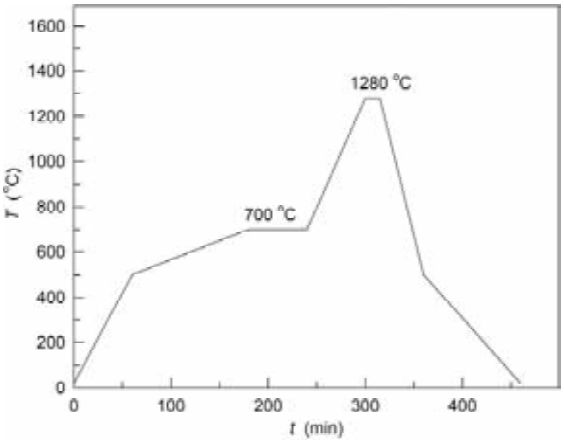

Fig. 1. Thermal theatment conditions used for sintering of WC - 8 wt.% Co hard alloys from different powder mixtures.

Nanocrystalline WC powder with mean particle size of 60 nm was produced by plasma-chemical reaction of tungsten oxide WO_3 with propane C_3H_8 in a low-temperature hydrogen plasma flow at a temperature of about 3500 °C with followed annealing of synthesized powder under argon at 800 °C.

The coarse-grained commercial WC powder was milled in a PM-200 Retsch planetary ball mill during 10 hours at 500 rotations per minutes in WC-Co grinding bowls using WC-Co balls. Conditions of ball milling are described in detail in [10,11].

Powder mixtures of WC-8wt.% Co were prepared by grinding one of mentioned above tungsten carbide powders with Co powder for 2 h. Hereinafter, the powder mixtures WC-8wt.% Co and the hard alloys produced will be designated for brevity as TC8-1 (ref) (standard powder mixture with mean particle size of 2 μm prepared by grinding of coarse-grained commercial WC powder with Co powder and the hard alloy sintered from this powder mixture), TC8-2 (powder mixture of submicrocrystalline commercial WC powder with Co powder and sintered hard alloy), TC8-3 (mixture of plasma-chemical WC nanopowder with Co powder and sintered hard alloy), and TC8-4 (mixture of ball-milled

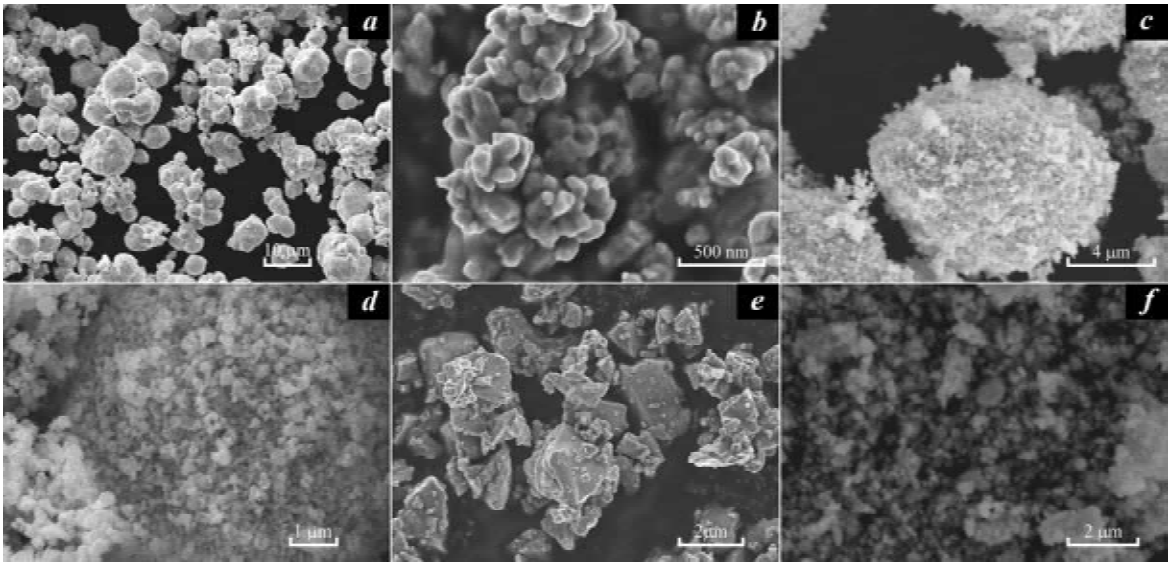

Fig. 2. Scanning electron microscopy of starting WC powders and WC-Co powder mixtures: (*a*) coarse-grained commercial tungsten carbide WC powder; (*b*) submicrocrystalline commercial tungsten carbide WC powder; (*c*) nanocrystalline WC powder, obtained by plasma-chemical method; (*d*) nanocrystalline WC powder, obtained by high-energy ball milling of coarse-grained WC powder; (*e*) coarse-grained reference TC8-1 powder mixture WC-Co; (*f*) nanocrystalline TC8-5 powder mixture WC-Co, obtained by ball milling of reference TC8-1 powder mixture.

nanocrystalline WC powder with Co powder and sintered hard alloy). One more TC8-5 powder mixture was produced by high-energy ball milling of the coarse-grained TC8-1 powder mixture in a PM-200 Retsch ball mill during 10 hours at 500 revolutions per minutes.

Green bulk rods with lengths of 40 mm and diameters of about 7 mm were prepared by cold-pressing the powder mixtures in a cylindrical steel die with small addition of ethanol. For all of the samples, the compaction pressure was 0.7 GPa.

The green rods were sintered in a vacuum of 10^{-2} Pa (~10^{-4} mm Hg). Fig. 1 presents thermal treatment sequence used for sintering of hard alloy rods. Maximum sintering temperature is equal to 1280 °C. It should be noted that the sintering temperature T_{sint} = 1280 °C is smaller than the eutectic temperature T_e = 1320 °C of the pseudobinary WC-Co system [12,13]. On the one hand, sintering at a temperature $T < T_e$ should provide the formation of homogeneous microstructure of hard alloys. On the other hand, sintering at $T < T_e$ allows to avoid strong recrystallisation of carbide phase because recrystallisation takes place in the presence of a liquid phase, i.e. at $T > T_e$. For details on the temperature-time condition of sintering see [14] also.

For comparison a rod from the ball-milled WC nanopowder without Co binder was sintered. Hereinafter, this WC rod is designated as WC (ball-milled).

The microstructure of the starting WC - Co powder mixtures and sintered hard alloys is examined by scanning electron microscopy (SEM) in JEOL 6310 (SCK-CEN) and LEO Gemini DSM982 (FELMI-ZFE, Graz) electron microscopes. Some SEM images are obtained in JEOL-JSM LA 6390 electron microscope equipped with EDX analyzer JED-2300.

All X-ray diffraction (XRD) measurements are performed in a DRON-UM1 diffractometer using Cu$K\alpha_{1,2}$ radiation at the angles 2θ between 10° and 140° in steps $\Delta 2\theta$ = 0.03° with the scan time of 2 s at each point. The mean size of the coherent scattering domains in fine-grained WC powders and nanostructured hard alloys is determined by an X-ray method from broadening of diffraction reflections [8,15]. The diffractometer instrumental angular resolution function $FWHM_R(2\theta) = (u\tan^2\theta + v\tan\theta + w)^{1/2}$ which is necessary for estimation of reflection broadening is determined in a special diffraction experiment with the cubic lanthanum hexaboride LaB_6 (NIST Standard Reference Powder 660a). The size of the particles and grains is evaluated also using the scanning electron microscopy (SEM). The particle size distribution in the WC powders is determined using a Laser Scattering Particle Size Distribution Analyzer HORIBA Partica LA-950V2.

Metallographic cross sections for the hard alloys microstructure analysis and Vickers hardness and microhardness measurements are prepared

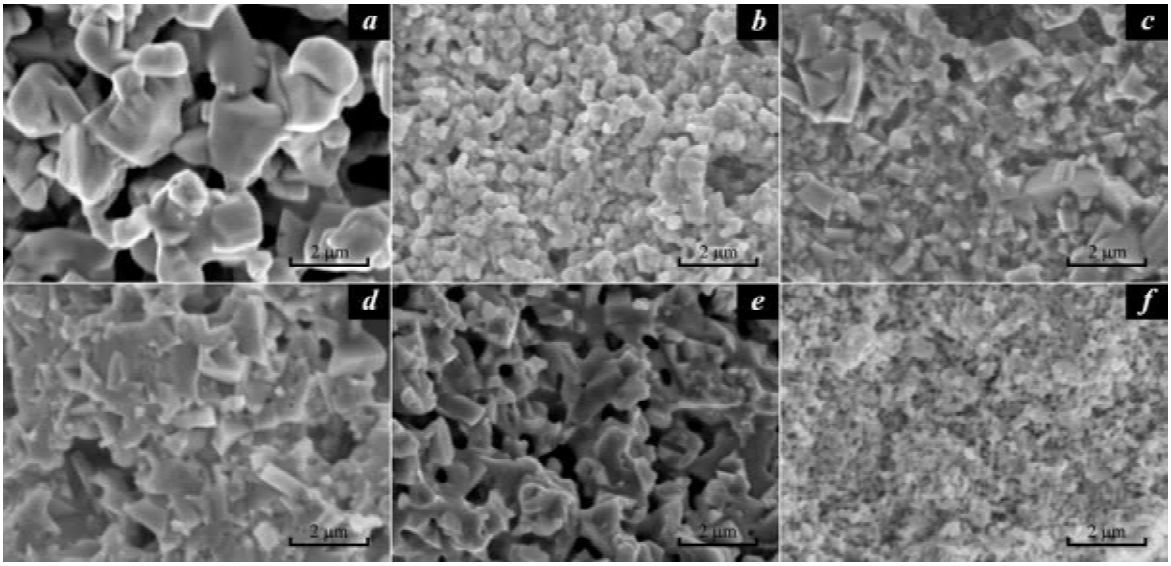

Fig. 3. Scanning electron microscopy of sintered hard alloys WC - 8wt.% Co and sintered pure tungsten carbide WC: (*a*) TC8-1 (ref) sintered from reference WC-Co powder mixture; (*b*) TC8-2 (smc-WC) sintered from powder mixture of Co and submicrocrystalline WC powder; (*c*) TC8-3 (plasma-WC) sintered from powder mixture of Co and nanocrystalline WC, obtained by plasma-chemical method; (*d*) TC8-4 (ball-milled WC) sintered from powder mixture of Co and nanocrystalline WC, obtained by ball milling; (*e*) TC8-5 (ball-milled WC-Co) sintered from ball-milled WC-Co powder mixture; (*f*) WC (ball-milled) sintered from ball-milled WC nanopowder without addition of Co.

using a metallographic BUEHLER setup. For exposure of grain boundaries the polished microsections are etched by the Murakami solution made from 10 g potassium hydroxide KOH, 10 g potassium ferricyanide $K_3Fe(CN)_6$, and 100 ml of H_2O. Vickers microhardness H_V was measured on diamond (1 mm oil suspension) polished specimens using a MICROMET-I microhardness testing machine with automatic loading. The indentation load was 1 N and the loading time was 10 s. The average values of H_V microhardness are obtained as the average of 20 measurements on each specimen. Vickers hardness *H* was measured under load 50 N using Wolpert hardness tester.

Bending strength is measured by means of three point bending tests with 18 mm distance between the support points using an INSTRON-1362 device. The cylindrical rods with length of 40 mm and diameter of about 7 mm are used for the measurements.

3. RESULTS AND DISCUSSION

The microstructure of the tungsten carbide powders used in this study is shown in Fig. 2. The coarse-grained WC powder consists of rounded and irregularly shaped agglomerates with mean size of 6 μm; these agglomerates consist of fine particles about 2 mm in size (Fig. 2a). There are many individual fine particles not larger than 1 mm in size; content of these particles in coarse-grained WC powder reaches 10-15 vol.%. The mean particle size of the submicrocrystalline WC powder (Fig. 2b) is equal to ~150 nm. Particles are strongly bonded to one another as if they were fused together. The WC powder produced by plasma-chemical synthesis has a microstructure (Fig. 2c) with well-observed large (up to 10 mm) loose agglomerates composed of smaller particles. The WC nanocrystalline powder prepared by ball milling has a microstructure (Fig. 2d) similar to plasma-chemical WC powder. However, the agglomerates in the ball-milled powder have a smaller size from 100 to 400 nm. According to the SEM data, the mean particle sizes in tungsten carbide nanopowders obtained by plasma-chemical synthesis (Fig. 2c) and by ball milling (Fig. 2d) are equal to 100 and 180 nm, respectively.

The mean particle size of the standard TC8-1 powder mixture is equal to 2 μm (Fig. 2e). Analysis of diffraction reflection broadening is shown that mean size of the coherent scattering regions is equal to 55±10 nm for the plasma-chemical WC nanocrystalline powder and 20±10 nm for the nanocrystalline powder produced by ball milling. The discrepancy in mean sizes observed by SEM and

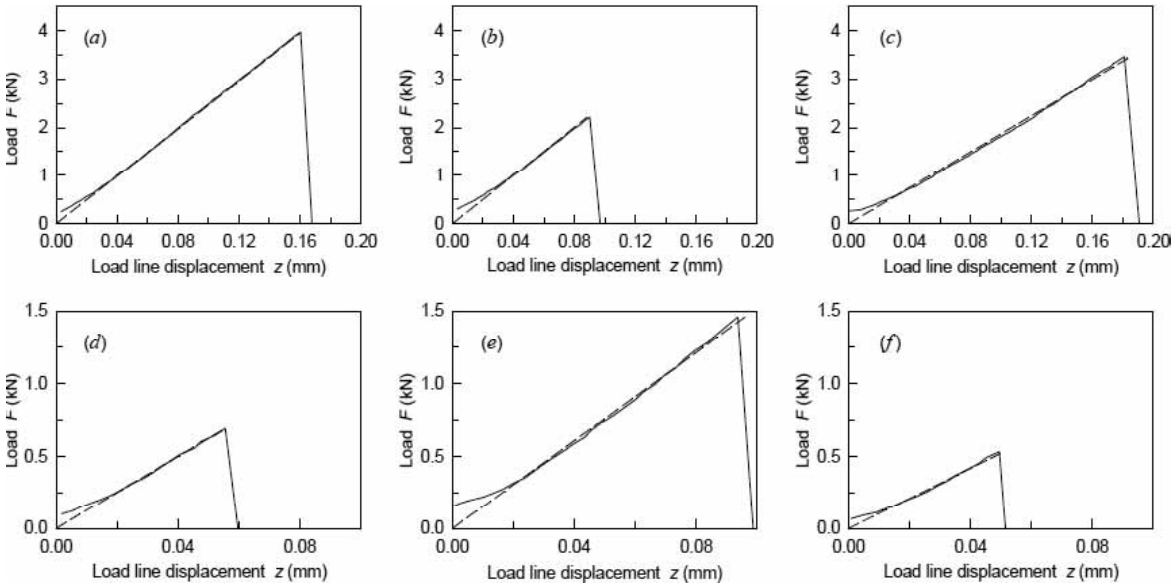

Fig. 4. Load plots $z(F)$ of the bending tests for cylindrical rods of WC - 8wt.% Co hard alloys and of WC specimen sintered without Co addition: (*a*) TC8-1 (ref), (*b*) TC8-2 (smc-WC), (*c*) TC8-3 (plasma-WC), (*d*) TC8-4 (ball-milled WC), (*e*) TC8-5 (ball-milled WC-Co), (*f*) WC (ball-milled).

XRD is evidence for a high degree of agglomeration of the powders. Thus, the coarse particles, up to several micrometers in size, observed by SEM are agglomerates of small particles with tens of nanometers in size.

A similar situation is observed for the TC8-5 powder mixture produced by ball milling of the standard TC8-1 powder mixture. According to SEM data (Fig. 2f) the mean particle size of the TC8-5 powder mixture is equal to about 180 nm and XRD analysis gives 20±10 nm.

SEM studies of a microstructure of sintered hard alloys (Fig. 3) show that the grain size for all WC-8wt.% Co alloys is larger in comparison with the WC particle size for starting powder mixtures. SEM images of the fracture surface of all sintered hard alloys after the bending tests present in Fig. 3.

Non-significant grain growth up to 3 μm is observed for hard alloy TC8-1 (Fig. 3a) sintered from standard powder mixture. The grain size of TC8-2 (smc-WC) hard alloy is about 450 nm (Fig. 3b) and increases in comparison with a particle size of starting powder. Hard alloys TC8-3 and TC8-4 prepared from plasma-chemical and ball-milled nanocrystalline WC powders have grains about 450 and 850 nm in size, respectively (Figs. 3c, 3d). It is larger than the particle size for starting WC powders but is one second – one third as much as grain size of TC8-1 hard alloy sintered from standard coarse-grained powder mixture. Mean grain size of TC8-5 hard alloy is ~900 nm (Fig. 3e). Thus the grain size of hard alloys is larger in comparison with the particle size of starting powders. In particular, this is the case for TC8-3, TC8-4 and TC8-5 hard alloys prepared from fine-grained powders (Figs. 3c, 3d, 3e). Apart from this, the grain size in specimen sintered from ball-milled nanocrystalline WC powder without cobalt addition is practically the same as the particle size in starting powder (Fig. 3f).

Fig. 3 shows that the microstructures of all sintered specimens are homogeneous. As is seen from Table, most fine-grained hard alloys are sintered from highly disperse powders.

Loading plots $z(F)$ obtained during the mechanical testing are presented in Fig. 4 for all six rods. In this figure z is displacement of neutral axis of rod and F is load which is normal to the neutral surface. Loading curves $z(F)$ are typical for brittle materials. Indeed, the failure of rod is observed at critical loading without preliminary plastic deformation. The fracture begins when a critical value of bending stress equal to bending strength σ_{bend} is attained. Modulus of elasticity in bending is proportional to $\Delta F/\Delta z$ ratio where Δz is a change of flexure value at load changing by ΔF value.

It is seen from Fig. 4 that the rods from TC8-1 (ref), TC8-2 (smc-WC) and TC8-3 (plasma-WC) hard alloys are more elastic in comparison with TC8-4, TC8-5 rods and rod from ball-milled tungsten carbide because flexure z values of the former rods are

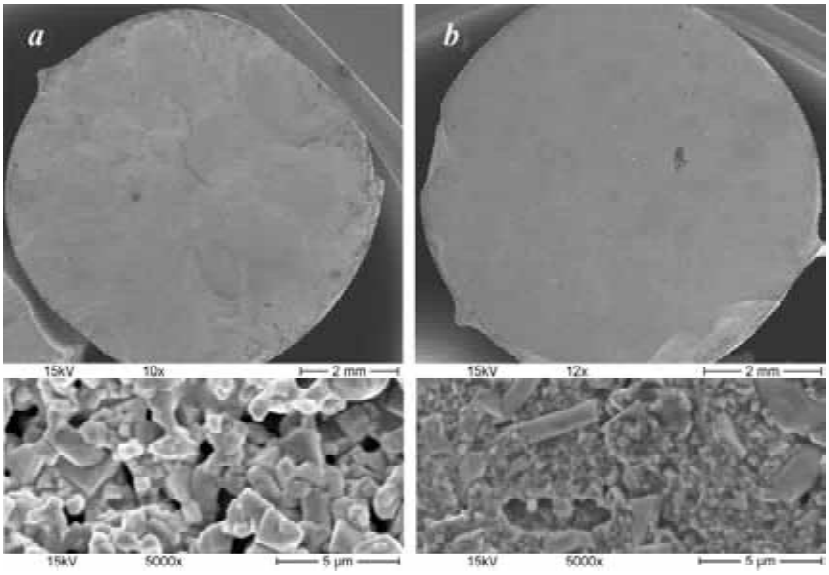

Fig. 5. SEM images of fracture surface of the rods produced from different WC - 8wt.% Co hard alloys: (*a*) the TC8-1 (ref) hard alloy, (*b*) TC8-3 (plasma-WC) hard alloy.

smaller than that of the latter rods at the same load *F*.

SEM images of fracture surface of the rods produced from TC8-1 (ref) and TC8-3 (plasma-WC) hard alloys are shown in Fig. 5. Both alloys have porosity about 10%. At a magnification of 10 times the fracture surface of TC8-1 hard alloys (Fig. 5a) represents a set of flat sections with small steps between them. Such element of a relief is named a "river" pattern and is characteristic for a macroscopic brittle failure [16]. In contrast to TC8-1 hard alloy, at the same magnification a fracture surface of the TC8-3 rod is smooth (Fig. 5b). It means that the TC8-3 hard alloy have at least microplasticity traces. Mean

Table 1. Properties of starting powders and sintered specimens (mean particle size or size of coherent scattering regions are given for the WC phase in the materials).

Specimen	Starting powders		Sintered alloys			
	Mean particle size according to SEM, nm	Mean particle size according to XRD, nm	Mean grain size according to SEM, nm	Vickers hardness, H±0.5,GPa	Micro-hardness, H_V±0.5,GPa	Bending strength, σ_{bend}±10, MPa
TC8-1 (ref)	2000	-	2500	12.5	11.6	480
TC8-2 (smc-WC)	150	-	500	-	13.1	280
TC8-3 (plasma-WC)	100	60	450	-	15.5	490
TC8-4 (ball-milled WC)	180	20	850	-	13.6	90
TC8-5 (ball-milled WC-Co)	180	20	900	-	16.6	190
WC(ball-milled)	180	20	180	16.8	16.0	70

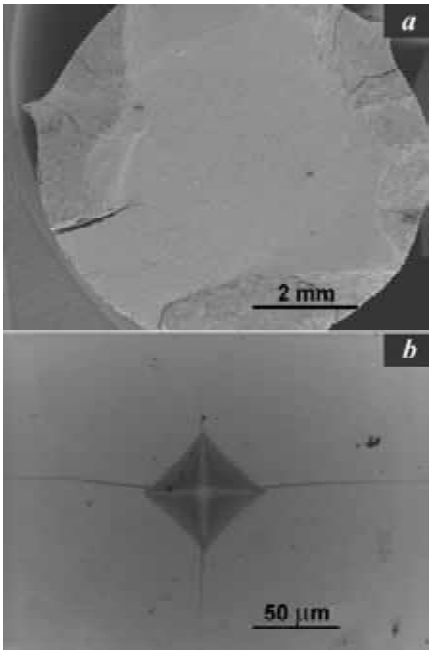

Fig. 6. Micrographs of the rod sintered ball-milled WC nanopowder without addition of Co: (*a*) SEM image of fracture surface of the rod, (*b*) optical image of indentation obtained by Vickers hardness test under load of 50 N.

grain size of TC8-1 hard alloy is equal to ~2 μm (Fig. 5a, bottom). Mean grain size of TC8-3 hard alloy is equal to 400-500 nm but there are separate large grains 1-2 mm in size (Fig. 5b, bottom).

According to [17], bending strength σ_{bend} of a cylindrical rod can be calculated using the formula

$$\sigma_{bend} = \frac{F_{fracture} LD}{8J}\left(1+\frac{4z^2}{L^2}\right) = \frac{F_{fracture} L}{\pi R^3}\left(1+\frac{4z^2}{L^2}\right). \quad (1)$$

where $F_{fracture}$ is the breaking load (force), $R = D/2$ is the radius of the transversal section of the rod, z is the flexure value, L is the distance between the support points, and $J = \pi R^4/4$ is the moment of inertia of the transversal section of a cylindrical rod. For brittle non-plastic materials value of flexure is negligibly small in comparison with L distance therefore the correction $(1 + 4z^2/L^2)$ can be neglected. In this case bending strength is

$$\sigma_{bend} = F_{fracture} D / 8J \equiv F_{fracture} L / \pi R^3. \quad (2)$$

The calculated σ_{bend} values for the six measured rods produced from all hard alloys are given in Table 1.

Fine-grained hard alloys have enough smooth fracture surfaces and at a large magnification one can only see that destruction of hard alloys occurs mainly along the grain interfaces. The WC (ball-milled) rod sintered from ball-milled nanocrystalline WC powder without Co addition has the lowest bending strength 70 MPa (Table 1). This is because tungsten carbide itself is a very brittle material. It is confirmed by the formation of cracks in the vertices of indentations obtained at measurements of hardness and the presence of chips and cracks on the fracture surface (Fig. 6).

Measuring hardness H at large load P allows estimating value of fracture toughness K_{1c} of sintered specimens from the hardness value and the length of cracks appearing in the indentation vertices. According to [18] fracture toughness is

$$K_{1c} = 0.016\left(E/H\right)^{1/2} P / l^{3/2}, \quad (3)$$

where E is Young's modulus and l is crack length measured from the center of indentation to the crack tip. We measured hardness H under load $P = 50$ N. The hardness H and mean crack length l for the specimen sintered from ball-milled nanocrystalline WC powder without Co-binder are equal to 16.8 GPa and 105 μm (see Fig. 6), respectively. The Young's modulus E of WC carbide is equal to ~700 GPa. Taking these values into account, the fracture toughness K_{1c} of WC (ball-milled) specimen sintered at 1280 °C is equal to about 5.0 MPa·m$^{1/2}$.

The TC8-3 hard alloy with uniform fine-grained microstructure has the highest bending strength σ_{bend} = 490 MPa closed to the σ_{bend} value of TC8-1 hard alloy. Confrontation of grain size with bending strength of TC8-2, TC8-3, TC8-4, and TC8-5 hard alloys finds out the correlation between these properties. The smallest values of bending strength σ_{bend} are observed for the TC8-4 and TC8-5 coarse-grained hard alloys whereas TC8-2 and TC8-3 hard alloys with smaller grain size have a larger bending strength (Table 1).

As is seen from Table 1, the highest microhardness H_V is observed for the TC8-5 hard alloy sintered from ball-milled nanocrystalline WC-Co powder mixture and the lowest one to the TC8-1 hard alloy prepared from the coarse-grained WC-Co powder mixture. All WC-Co hard alloys sintered from nanocrystalline WC powders have higher microhardness than hard alloy sintered from coarse-grained WC powder. Even though the difference is small, this fact shows the need for further investigations of hard alloys prepared from nanocrystalline powders.

4. CONCLUSION

Decreasing the particle size of starting WC powders down to nanosize leads to a more fine homogeneous structure of sintered hard alloys. WC-Co hard alloys obtained from nanocrystalline WC powders have a higher microhardness than alloys prepared from coarse-grained or submicrocrystalline WC powders. Relation of the grain size to bending strength of hard alloys is not so ambiguous. For example, cobalt free specimen sintered from ball-milled nanocrystalline WC powder has higher hardness and preserves the small grain size about 180 nm even after high-temperature sintering at 1280 °C, but it is very brittle and has low bending strength. Thus, the small grain size itself is not a sufficient condition for good mechanical properties of hard alloys.

ACKNOWLEDGEMENTS

This work is supported by the Russian Foundation for Basic Research (grant 10-03-00023a) and the Ural Division of the Russian Academy of Sciences (project No 10-3-11-UT). Authors are grateful to L. van Houdt (SCK-CEN, NMS Institute, Mol, Belgium) for performing bending tests and A.I. Gusev for helpful discussion.

REFERENCES

[1] A.I. Gusev, A.A. Rempel and A.J. Magerl, *Disorder and Order in Strongly Nonstoichiometric Compounds: Transition Metal Carbides, Nitrides and Oxides* (Springer, Berlin - Heidelberg - New York - London, 2001).

[2] A.I. Gusev, *Nonstoichiometry, Disorder, Short-Range and Long-Range Order in Solids* (Nauka, Moscow, 2007). (*in Russian*)

[3] J.H. Westbrook, E.R. Stover, In: *High-Temperature Materials and Technology*, ed. by I.E. Campbell and E.M. Sherwood (Wiley, New York, 1967) pp.312-348.

[4] H.O. Pierson, *Handbok of Refractory Carbides and Nitrides. Properties, Characteristics, Processing and Applications* (Nova Publications, Westwood, 1996).

[5] G.S. Upadhyaya, *Nature and Properties of Refractory Carbides* (Nova Science Publishers, New York, 1996).

[6] R. Kieffer and F. Benesovsky, *Hartmetalle* (Springer, Wien - New York, 1965).

[7] W. Schedler, *Hartmetall für den Praktiker: Aufbau, Herstellung, Eigenschaften und industrielle Anwendung einer modernen Werkstoffgruppe* (VDI-Verlag, Düsseldorf, 1988).

[8] A.I. Gusev and A.A. Rempel, *Nanocrystalline Materials* (Cambridge Intern. Science Publ., Cambridge, 2004).

[9] *Nanostructures: Synthesis, Functional Properties and Applications* (NATO Science Series II: Mathematics, Physics and Chemistry. V.128) Ed. by T. Tsakalakos, I.A. Ovid'ko and A.K. Vasudevan (Kluwer Academic Publishers, Dordrecht - Boston - London, 2003).

[10] A.S. Kurlov and A.I. Gusev // *Technical Physics Letters* **33** (2007) 828.

[11] A.I. Gusev and A.S. Kurlov // *Nanotechnology* **19** (2008) paper 265302, 1.

[12] P. Rautala and J.T. Norton // *Transact. AIME* **194** (1952) 1045.

[13] A.F. Guillermet // *Metallurg. Transact. AIME A* **20A** (1989) 935.

[14] A.S. Kurlov and A.A. Rempel // *Inorganic Materials* **43** (2007) 602.

[15] G.K. Williamson and W.H. Hall // *Act. Metal*. **1** (1953) 22.

[16] J.L. McCall, H. Steele, *Practical application of quantitative metallography* (ASTM International, Philadelphia, 1984).

[17] S. Timoshenko, *Strength of Materials, part 1, Elementary Theory and Problems*, second ed., (D. Van Nostrand Company, Princeton, 1940).

[18] G.R. Anstis, P. Chantikul, B.R. Lawn and D.B. Marshall // *J. Am. Ceram. Soc*. **64** (1981) 533.